Journal of Physical Science, Vol. 34(1), 43–55, 2023

Electroplated ZnO Thin Film: Influence of Deposition Time on Optical and Structural Properties

Nurdin Siregar*, Motlan and Makmur Sirait

Department of Physics, Faculty of Mathematics and Natural Sciences, Universitas Negeri Medan, Jalan Willem Iskandar Medan Estate, Medan 20221, Indonesia

*Corresponding authors:siregarnurdin@unimed.ac.id

Published online: 28 April 2023

To cite this article: Siregar, N. et al. (2023). Electroplated ZnO thin film: Influence of deposition time on optical and structural properties. *J. Phys. Sci.*, 34(1), 43–55. https://doi.org/10.21315/jps2023.34.1.4

To link to this article: https://doi.org/10.21315/jps2023.34.1.4

ABSTRACT: *Zinc oxide (ZnO) thin film, an important n-type semiconductor for various applications, needs to be prepared by a simple and low-cost method. Herein, ZnO thin films with various deposition times (1.25 min, 2.50 min, 5.00 min and 7.5 min) have been successfully fabricated by the electroplating method. The X-ray diffraction analysis demonstrates that the crystal structure of all samples was hexagonal, with the largest crystal size of 28.17 nm and a deposition time of 2.50 min. The scanning electron microscopy (SEM) analysis shows that the deposition time increased along with the more visible size distribution of the crystallite grains and the smaller, more spherical and uniform, compact coating of the substrate. It is found that increasing the deposition time from 1.25 min to 7.5 min leads to an increment of thickness from 0.84 μm to 4.4 μm. The elemental analysis reveals the presence of zinc (Zn) and oxygen (O) without impurities. The optical analysis reveals that the ZnO transmittance was greater than 95% for all deposition times. The highest bandgap energy value of the ZnO thin film is 3.24 eV at a deposition time of 1.25 min. With great optical and structural properties, our ZnO thin film has a big potential to be used for dye-sensitised solar cells (DSSC).*

Keywords: ZnO thin film, deposition time, electroplating method, opticical, structural

1. INTRODUCTION

The development of zinc oxide (ZnO) thin film semiconductors has rapidly progressed in the last few decades. As an n-type semiconductor from Group II-VI, ZnO is widely used in organic solar cells and dye-sensitised solar cells (DSSC)

due to its low cost, ease of synthesis, non-toxicity, high stability and excellent optoelectronic properties.[1,2] In addition, ZnO has multifunctional properties with high energy binding strength, low resistivity and large light-capturing properties, making it one of the most promising thin film materials for various applications.[3,4]

It is well known that ZnO thin films can be prepared using physical vacuum technology, including, radio frequency (RF) magnetron sputtering, direct current (DC) sputtering, pulsed laser deposition (PLD) and electron-beam evaporation techniques.[5–9] However, these techniques have the disadvantage of necessitating the use of expensive pumps to vacuum the chamber. In contrast, the chemical method is more attractive and promising for preparing thin films because of its low-cost and the lack of a particular apparatus. Therefore, electrochemical or electroplating techology appears to be an alternative method for preparing ZnO thin film. There are many parameters that can be tuned during the electroplating in order to obtain the optimal properties. The advantages of electroplating over other techniques are low temperature process, the simple and inexpensive equipment, the lack of need for a vacuum chamber, time-efficiency and low energy consumption.[10,11]

Based on the previous study, the variations in potential affect the morphology of ZnO.[12] They also found that the higher the applied potential during electrodeposition, the lower the resistance value. The most suitable coating for DSSC was coating at potential –1.0 V. Other studies have shown that deposition time has a significant impact on the crystal size, layer thickness and resistivity of thin films.[13,14] Similarly, Shafi et al. discovered that increasing the deposition time increases crystallite size and bandgap energy.[15] In this work, the influence of various deposition times on the structural and optical properties of the ZnO thin films prepared by electroplating method with a two-electrode system is systematically investigated.

2. EXPERIMENTAL

2.1 Materials and Synthesis Procedures

Zinc metal (Alfa Aeasar, 98%), ZnSO4 (Alfa Aeasar, 99%) and ITO glass (Sigma-Aldrich) were purchased from Indonesia and used in this study for growing ZnO thin film by electroplating technique. To prepare the electrolyte solution for electroplating, about 1.61 g of ZnSO4 was dissolved into 50 ml of Deionised (DI) water. The ZnO thin films were manufactured by the electroplating method using a potentiostat with a deposition current of 10 mA/cm2 and deposition time

variations (1.25 min, 2.50 min, 5.00 min and 7.5 min). ITO glass and zinc metal are placed parallel to each other and are used as the working electrode and counter electrode, respectively. After drying, the sample was heated up in a furnace at temperature 500ºC for 2 h to form a ZnO thin film.

2.2 Characterisation Tools

X-ray diffractometer (LabX XRD-6100, Shimadzu) was conducted to investigate the structural properties in Indonesia. A scanning electron microscope (JEOL-6500) was used for recording the surface and cross section images in Taiwan. Both transmittance and absorbance spectra were studied using a UV-Vis NIR spectrophotometer in Indonesia. A VG ESCA Scientific Theta Probe was used x-ray photoelectron spectroscopy analysis in Taiwan.

3. RESULTS AND DISCUSSION

3.1 X-ray Analysis

Figure 1 shows x-ray diffraction pattern (XRD) of ZnO thin film for variation deposition times of 1.25 min, 2.50 min, 5.00 min and 7.50 min together with pure indium tin oxide (ITO) glass. The analysis of x-ray diffraction patterns reveals that all samples have similar peak positions at 32.1º, 34.3º and 36.5º that reveal formation of ZnO with (100), (002) and (101) planes, respectively, according to the standard file PDF# 36-1451 for ZnO hexagonal structure. The other peak at about 21.45, 30.54, 35.41, 37.64, 41.78, 45.62, 50.95 and 55.90 is contributed by the ITO substrate, which well agrees with the standard file PDF# 89-4958 (Indium Tin Oxide, ITO). All the ZnO thin films also have same preferantion growth peak of (101) plane.[16] This result also shows that the deposition time does not change the crystal structure.

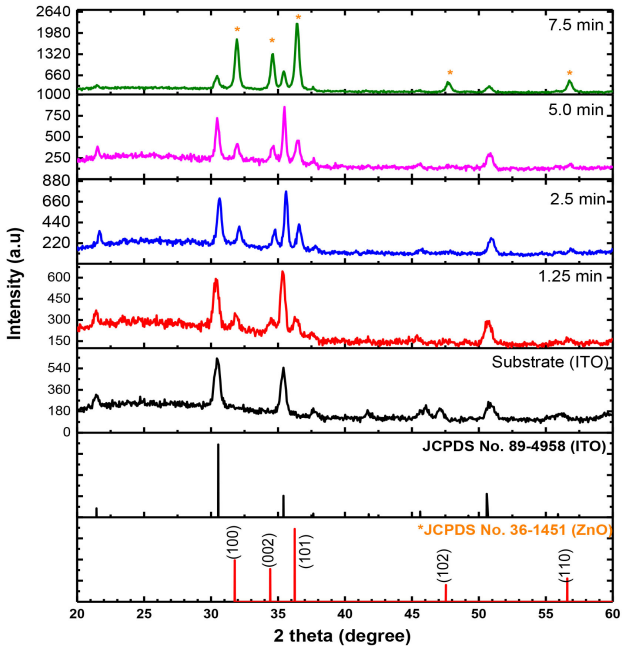

Figure 1: XRD pattern of ZnO Thin Film at various deposition time: (a) 1.25 min, (b) 2.50 min, (c) 5.00 min and (d) 7.5 min.

The average crystallite size of the ZnO is then obtained using the Scherrer formula [Equation (1)], as listed in Table 1.[17]

$$D = \frac{\theta.9\lambda}{\beta \cos \theta} \quad (1)$$

It is noted that average crystallite size depends on the value of Full-Width at Half Maximum (FWHM) or the width of the XRD peak. If the value of FWHM is small, then the average crystallite size is large, and vice versa. Based on Table 1 it can be seen that the average crystallite size increased with increasing deposition time up to 2.50 min. This result is in accordance with earlier results which, also found that as the deposition time takes longer the average crystallite size also increases.[18,19] Furthermore, the average crystallite size started to decrease when the deposition time was increased to 5.00 min and 7.50 min, respectively. The largest average crystallite size was 28.17 nm at a deposition time of 2.50 min. This result is in accordance with the previous work, which stated that the average crystal size decreased with increasing deposition time.[20] According to Winarka et al., with variations in deposition time, the result is the largest average crystal size at the

deposition time of 25 s and decreases when the deposition time increases.[21] The average crystallite size of the sample decreased with increasing deposition time due to accumulation in the form of agglomeration on the surface of the sample.[22] The dislocation density, lattice spacing, and macro strain values of our samples were also computed and listed in Table 1.

Table 1: Average crystallite size, dislocation density, lattice spacing and macrostrain values of ZnO thin films at different deposition times.

Time (min)	Average crystallite size (nm)	Dislocation density x 10^{-3} (nm^{-2})	Lattice spacing (Å)	Macro strain values <e>
1.25	24.81	1.63	2.472	1.45 x 10^{-3}
2.5	28.17	1.26	2.453	9.36 x 10^{-3}
5.0	27.65	1.31	2.460	6.21 x 10^{-3}
7.5	26.93	1.38	2.464	4.89 x 10^{-3}

3.2 Morphology and Thickness

The morphological of ZnO thin film growth at various deposition time was recorded by a field emission scanning electron microscope, as illustrated in Figure 2. The SEM images exhibit that the morphological of samples is affected by deposition time. The average particle sizes based on those SEM images were 38 ± 9 nm, 51 ± 12 nm, 60 ± 15 nm and 99 ± 33 nm for deposition times of 1.25 min, 2.5 min, 5.0 min and 7.5 min, respectively. The increase in deposition time is accompanied by a more visible distribution of larger and more compact grains that cover the substrate. It occurs because the atoms in the smaller grains are energetic enough to diffuse and form a larger grain.[23] As a result of this diffusion between grains, necking will form, which causes the boundary between grains and porosity to contract, resulting in a smoother appearance on the surface of the thin film. It is observed that the deposition time increases as the number of atoms in a crystal increases, indicating that the quality of the crystal improves.

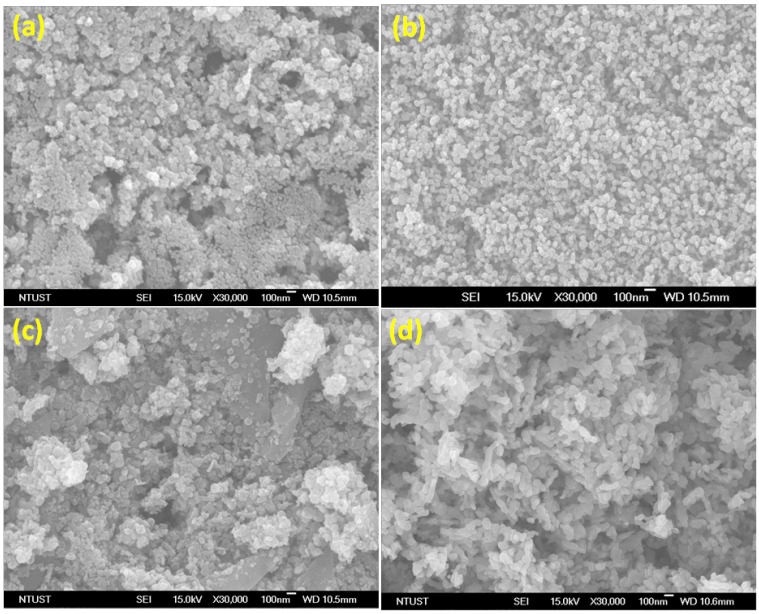

Figure 2: SEM images of the surface ZnO thin film at various deposition times: (a) 1.25 min, (b) 2.50 min, (c) 5.00 min and (d) 7.5 min.

To investigate the effect of the deposition time on the thickness of the ZnO thin film, the SEM analysis was recorded on the cross section of the samples. As shown in Figure 3, the layer coating of ZnO thin film consistently thicken with increasing the deposition time from 1.25 min to 7.5 min. The actual thickness was then estimated based on the scale bar provided in each image. The thickness of ZnO thin films were 0.84 µm, 2.04 µm, 2.92 µm and 4.4 µm for deposition times of 1.25 min, 2.5 min, 5.0 min and 7.5 min, respectively.

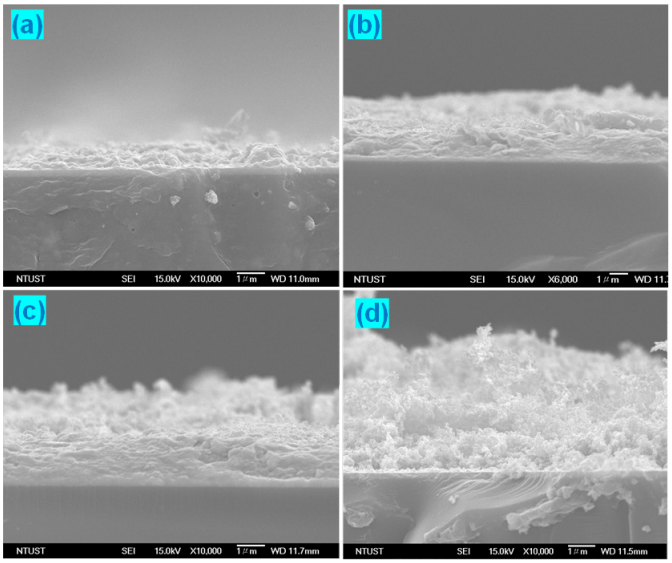

Figure 3: Cross section SEM images of the ZnO thin film at various deposition times: (a) 1.25 min, (b) 2.50 min, (c) 5.00 min and (d) 7.5 min.

3.3 EDS Analysis

To determine the atomic percentages of each element contained in the samples, the EDS analysis was conducted, as presented in Figure 4.

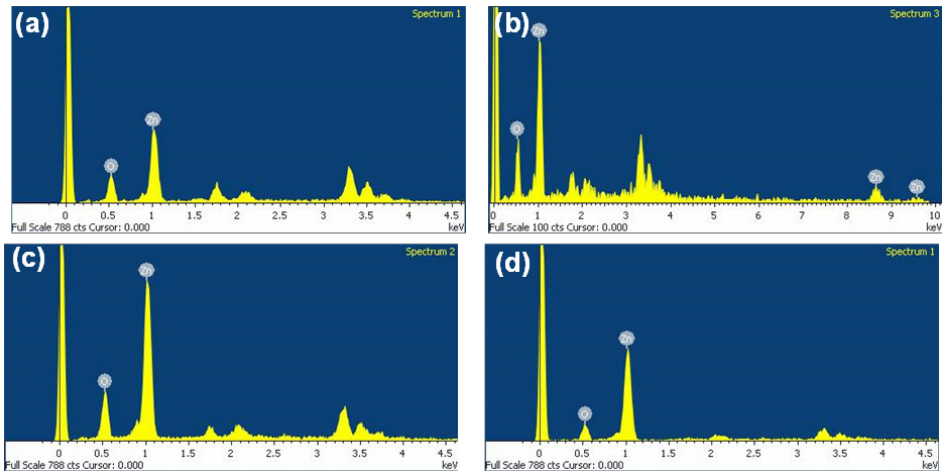

Figure 4: EDS spectra of of ZnO at various deposition times: (a) 1.25 min, (b) 2.50 min, (c) 5.00 min and (d) 7.5 min.

Table 2 lists the percentages of zinc (Zn) and oxygen (O) in the sample based on the peak area in Figure 4 with varying deposition times (1.25 min, 2.50 min, 5.00 min and 7.50 min), 0.2 M solution concentration, and 10 mA deposition current. The highest concentration of Zn was 52.44% at 7.50 min, while the lowest concentration was 38.76% at 1.25 min. The proportion of O in a ZnO thin film decreases as deposition time increases. The highest O percentage was 61.24% at 1.25 min and the lowest was 47.56% at 7.50 min. This EDS analysis revealed that the deposition time affected the proportions of Zn and O in ZnO.

Table 2: Atomic percentages of ZnO thin film at various deposition times.

Times (min)	Zn (%)	O (%)
1.25	38.76	61.24
2.50	40.15	59.85
5.00	42.79	57.21
7.50	52.44	47.56

3.4 XPS Analysis

ZnO thin film that has been fabricated with a deposition time of 7.5 min was analysed using x-ray photoelectron spectroscopy to investigate the oxidation state of Zn and O. Figure 5(a) shows the high-resolution XPS spectrum of Zn 2p. It can be seen that the Zn 2p has doublet peaks at binding energies of 1,020.1 eV and 1,043.1 eV, which corresponding to the Zn $2p_{1/2}$ and Zn $2p_{3/2}$, respectively.[24] These values confirm that Zn has the bivalent state. Figure 5(b) demonstrates the XPS spectrum of O1s. The ansymeteric peak indicates the presence of more than one peak. Therefore, after the deconvolution technique, there are two peaks with binding energies of 528.7 eV and 530.5 eV that reveal the presence of O lattice and O vacancy, respectively.[25]

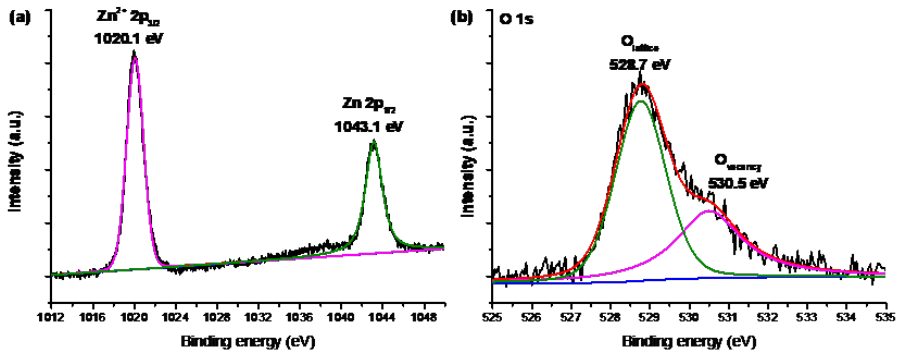

Figure 5: High-resolution XPS spectra of (a) Zn and (b) oxygen.

3.5 Optical Properties of ZnO Thin Film

To evaluate the optical properties of all samples, the transmittance and absorbance spectra were recorded using a UV-Vis spectrophotometer at wavelength of 200 nm–600 nm, as exhibited in Figure 6. Figure 6(a) demonstrates that the absorbance of all samples sharply drops at a wavelength of about 300 nm–390 nm, which corresponds to the ultraviolet wavelength region. Prolonging the deposition time shifts the absorption edge towards a shorter wavelength. Figure 6(b) depicts the transmittance spectra of ZnO at various deposition time, revealing a significant enhancement at wavelength between 365 nm and 400 nm. As deposition time increases, the transmittance values decrease. This is due to the fact that the longer the deposition time, the more atoms will be coated on the substrate, leading to the collisions between light and particles atoms more frequently and more difficult for light to pass through. All ZnO thin film samples possess a transmittance value reater than 95%, allowing them to be utilised in solar cells. The high transmittance value of the thin film is excellent and suitable for solar cell applications.

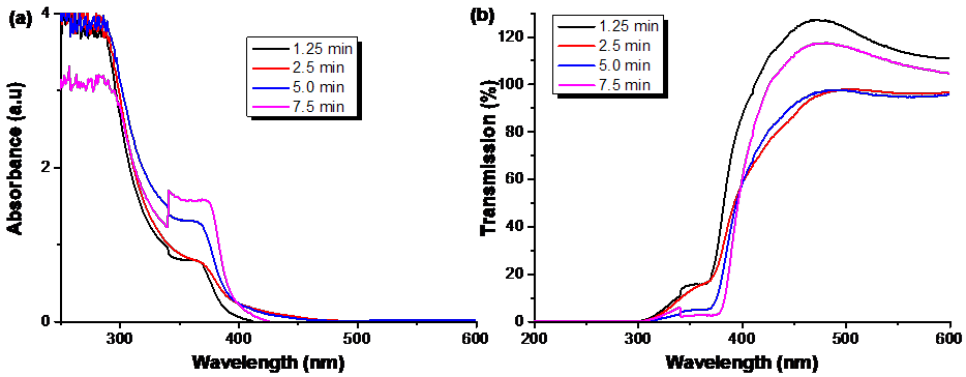

Figure 6: (a) Absorbance and (b) transmittance spectrum of ZnO at various deposition times.

The direct band gap energy value can be estimated based on the relationship of the absorbance and the photon energy, as demonstrated in Equation (2).[26]

$$(\alpha hv)^2 = C_D(hv - E_{opt}) \tag{2}$$

Figure 7, illustrates the Tauct plot of all samples with variations in deposition times.

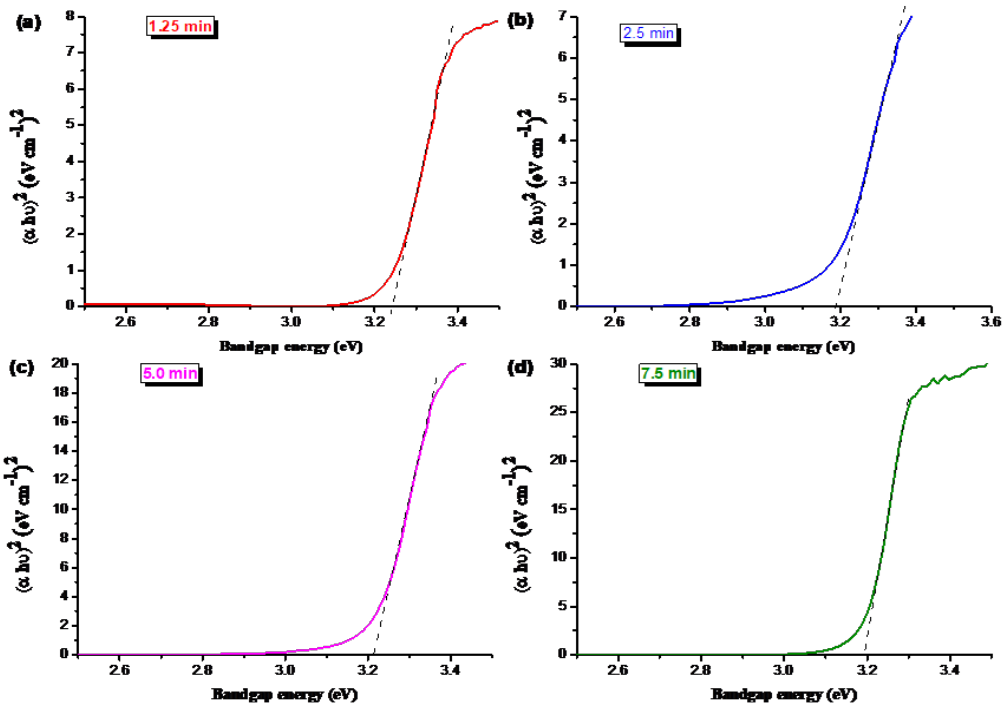

Figure 7: Tauc Plot Bandgap energy of ZnO at various deposition times: (a) 1.25 min, (b) 2.50 min, (c) 5.00 min and (d) 7.50 min.

The bandgap energy of ZnO thin films with varying deposition times is shown in Table 3 based on Tauc Plot in Figure 7.

Table 3: Bandgap energy ZnO at various deposition times.

Time (min)	Bandgap (eV)
1.25	3.24
2.50	3.19
5.00	3.21
7.50	3.19

It can be observed that the deposition time increases as the energy band gap decreases. The value of the largest energy band gap is at 1.25 min deposition time. According to previous studies, the energy band gap increased with prolonged

deposition times.[18,27] This demonstrates that prolonging deposition time results in a greater number of constituent atoms, which increases the energy absorbed by the material and decreases the energy band gap. The band gap energy decreament related to larger crystal size value, this result is consistent with early report.[28]

4. CONCLUSION

By electroplating, ZnO thin films with varying deposition times have been successfully synthesised. Thin film average crystallite size ranges from 24.81 nm–28.17 nm, with a maximum of 28.17 nm at 2.50 min of deposition. ZnO thin film has two peaks, Zn 2p and O 1s, with respective binding energies of 1,020 eV and 529 eV. The deposition time influences the size distribution of the spherical and uniform crystallite grains. The deposition time influences the percentages of Zn and O in ZnO, with the deposition time increasing as the percentage of Zn increases and decreasing as the percentage of O in the ZnO thin film decreases. UV-Vis analysis revealed that the transmittance value of the ZnO thin film was greater than 95% for all deposition times. The band gap energy values of ZnO thin films ranged from 3.19 eV to 3.24 eV, with a maximum value of 3.24 eV at 1.25 min of deposition time.

5. ACKNOWLEDGEMENTS

This research is sponsored ministry of education of the republic of Indonesia under grant number 021/UN33.8/DRTPM/PL/2022. The authors thank the rector of the Universitas Negeri Medan.

6. REFERENCES

1. Fattah, Z. A. (2016). Synthesis and characterization of nickel doped zinc oxide nanoparticles by sol–gel method. *Int. J. Eng. Res. Technol.*, 3, 2277–9655. http://doi.org/10.5281/zenodo.56998
2. Siregar, N. et al. (2022). Synthesis and optical properties of Sb-doped ZnO thin film by Sol-gel coating method. *J. Phys. Conf. Ser.*, 2193, 012063. https://doi.org/10.1088/1742-6596/2193/1/012063
3. Caglar, Y. et al. (2009). Crystalline structure and morphological properties of undoped and Sn doped ZnO thin films. *Superlattices microstruc.*, 46(3), 469–475. https://doi.org/10.1016/j.spmi.2009.05.005
4. Saravanakumar, M. et al. (2014). Effect of annealing temperature on characterization of ZnO thin films by sol-gel method. *Int. J. Chemtech Res.*, 6(5), 2941–2945. https://www.sphinxsai.com/2014/vol6pt5/5/(2941-2945)S-2014.pdf

5. Wang, C. et al. (2022). Structural, optical and half-metallic properties of Mn and As co-implanted ZnO thin films. *App. Surf. Sci.*, 575, 151703. https://doi.org/10.1016/j.apsusc.2021.151703
6. Aida, M. S. et al. (2022). Impact of samarium on the structural and physical properties of sputtered ZnO thin films. *Optik*, 250(1), 168322. https://doi.org/10.1016/j.ijleo.2021.168322
7. Cachoncinlle, C. et al. (2022). Anisotropy of physical properties in pulsed laser-deposited ZnO films. *Appl. Phy. A.*, 128(6), 1–10. https://doi.org/10.1007/s00339-022-05633-7
8. Ikhmayies, S. J. (2021). A study of the absorption edge of ZnO thin films prepared by the spray pyrolysis method. In S. J. Ikhmayies (Ed.). *Characterization of Minerals, Metals, and Materials 2021*. New York: Springer, 83–92. https://doi.org/10.1007/978-3-030-65493-1_8
9. Mohammed, R. et al. (2020). Synthesis and characterizations of ZnO thin films grown by physical vapor deposition technique. *J. Appl. Sci. Technol. Trends*, 1(4), 135–139. https://doi.org/10.38094/jastt1456
10. Khelladi, M. R. et al. (2013). A study on electrodeposited zinc oxide nanostructures. *J. Mater. Sci.: Mater. Electron.*, 24(1), 153–159. https://doi.org/10.1007/s10854-012-0973-5
11. Li, J. et al. (2020). Zinc interstitial and oxygen vacancy mediated high Curie-temperature ferromagnetism in Ag-doped ZnO. *Ceram. Inter.*, 46(11), 18639–18647. https://doi.org/10.1016/j.ceramint.2020.04.176
12. Elsayed, E. M. et al. (2014). Preparation of ZnO nanoparticles using electrodeposition and co-precipitation techniques for dye-sensitized solar cells applications. *J. Mater. Sci. Mater. Electron.*, 25(8), 3412–3419. https://doi.org/10.1007/s10854-014-2033-9
13. Tlemçani, T. S. et al. (2015). Deposition time effect on the physical properties of Cu_2ZnSnS_4 (CZTS) thin films obtained by electrodeposition route onto Mo-coated glass substrates. *Ener. Proced.*, 84, 127–133. https://doi.org/10.1016/j.egypro.2015.12.305
14. Anand, T. J. S. et al. (2018). Influence of deposition time on electrodeposited nickel selenide ($NiSe_2$) thin films for solar/photoelectrochemical cells. *J. Adv. Manuf. Technol.*, 12(1), 111–124. https://jamt.utem.edu.my/jamt/article/view/4902/3600
15. Shafi, M. A. et al. (2022). Optimization of electrodeposition time on the properties of Cu_2ZnSnS_4 thin films for thin film solar cell applications. *Opt. Quantum Electron.*, 54(8) 1–13. https://doi.org/10.1007/s11082-022-03913-3
16. Gultom, N. S. et al. (2020). Phase transformation of bimetal zinc nickel oxide to oxysulfide photocatalyst with its exceptional performance to evolve hydrogen. *Appl. Catal. B*, 272, 118985. https://doi.org/10.1016/j.apcatb.2020.118985
17. Gultom, N. S. et al. (2022). Bimetallic cobalt–nickel electrode made by a sputtering technique for electrocatalytic hydrogen evolution reaction: Effect of nickel ratios. *ACS Appl. Ener. Mat*., 5(7), 8658–8668. https://doi.org/10.1021/acsaem.2c01177

18. Yaw, C. S. et al. (2016). Effect of deposition time on the photoelectrochemical properties of cupric oxide thin films synthesized via electrodeposition method. *MATEC Web Conf.*, 60, 01001. https://doi.org/10.1051/matecconf/20166001001
19. Mulyadi, M. (2022). The effects of deposition time on phase and structure of FeCoNi films. *Chem. Mater.*, 1(2), 40–44. https://doi.org/10.56425/cma.v1i2.23
20. Karim, N. A. et al. (2018). Effects of deposition time on cobalt sulfide thin film electrode formation. *Malaysian J. Anal. Sci.*, 22(1), 80–86. https://doi.org/10.17576/mjas-2018-2201-10
21. Wijanarka, W. A., & Toifur, M. (2020). Effect of deposition voltage on layer thickness, microstructure, Cu/Ni sheet resistivity of deposition results by magnetic field electroplating assisted technique. *Indonesian Rev. Phys.*, 3(1), 23–29. https://doi.org/10.12928/irip.v3i1.1530
22. Temel, S. et al. (2017). Effects of deposition time on structural and morphological properties of synthesized ZnO nanoflowers without using complexing agent. *Eur. Sci. J.*, 9, 13–27. http://doi.org/10.19044/esj.2017.v13n27p28
23. Shin, K. S. Et al. (2012). High quality graphene-semiconducting oxide heterostructure for inverted organic photovoltaics. *J. Mat. Chem.*, 22(26), 13032–13038. https://doi.org/10.1039/C2JM00072E
24. Gultom, N. S. et al. (2021). Transforming Zn (O, S) from UV to visible-light-driven catalyst with improved hydrogen production rate: Effect of indium and heterojunction. *J. Alloys Compd.*, 869, 159316. https://doi.org/10.1016/j.jallcom.2021.159316
25. Karamat, S. et al. (2022). Chemical interactions of nano islandic graphene grown on titanium dioxide substrates by chemical vapor deposition. *Arab J. Sci. Eng.*, 47(6), 7779–7788. https://doi.org/10.1007/s13369-022-06674-z
26. Abdullah, H. et al. (2020). Effects of tin in La–Sn-Codoped Zn (O, S) photocatalyst to strongly cleave the Azo bond in Azobenzene with in situ generated hydrogen. *ACS appl. Mat. Interf.*, 12(14), 16186–16199. https://doi.org/10.1021/acsami.9b19885
27. Damisa, J. et al. (2021). Deposition time induced structural and optical properties of lead tin sulphide thin films. *J. Niger. Soc. Phys. Sci.*, 3(4) 455–458. https://doi.org/10.46481/jnsps.2021.157
28. Kumar, M., Sasikumar, C. (2014). Electrodeposition of Nanostructured ZnO Thin Film: A Review. *Am. J. Mater. Sci.* 2(2), 18–23. https://doi.org/0.12691/ajmse-2-2-2